

Effect of cosmic backreaction on the future evolution of an accelerating universe

Nilok Bose* and A. S. Majumdar†

S. N. Bose National Centre for Basic Sciences, Block JD, Sector III, Salt Lake, Kolkata 700098, India

(Dated: February 16, 2019)

We investigate the effect of backreaction due to inhomogeneities on the evolution of the present universe by considering a two-scale model within the Buchert framework. Taking the observed present acceleration of the universe as an essential input, we study the effect of inhomogeneities in the future evolution. We find that the backreaction from inhomogeneities causes the acceleration to slow down in the future for a range of initial configurations and model parameters. The present acceleration ensures formation of the cosmic event horizon, and our analysis brings out how the effect of the event horizon could further curtail the global acceleration, and even lead in certain cases to the emergence of a future decelerating epoch.

PACS numbers: 98.80.-k, 95.36.+x, 98.80.Es

I. INTRODUCTION

The present acceleration of the Universe is well established observationally [1], but far from understood theoretically. The simplest possible explanation provided by a cosmological constant is endowed with several conceptual problems [2]. Alternative scenarios based on mechanisms such as modification of the gravitational theory and invoking extra fields invariably involve making unnatural assumptions on the model parameters, though there is no dearth of innovative ideas to account for the present acceleration [3]. The present state of knowledge offers no clear indication on the nature of the big rip that our Universe seems to be headed for.

Observations of the large scale universe confirm the existence of matter inhomogeneities up to the scales of superclusters of galaxies, a feature that calls for at least an, in principle, modification of the cosmological framework based on the assumption of a globally smooth Friedmann–Robertson–Walker (FRW) metric. Taking the global average of the Einstein tensor is unlikely to lead to the same results as taking the average over all the different local metrics and then computing the global Einstein tensor for a nonlinear theory such as general relativity. This realization has led to investigation of the question of how backreaction originating from density inhomogeneities could modify the evolution of the universe as described by the background FRW metric at large scales.

In recent times there is an upsurge of interest on studying the effects of inhomogeneities on the expansion of the Universe. The main obstacle to this investigation is the difficulty of solving the Einstein equations for an inhomogeneous matter distribution and calculating its effect on the evolution of the Universe through tensorial averaging techniques. Approaches have been developed to calculate the effects of inhomogeneous matter distribution on

the evolution of the Universe, such as Zalaletdinov’s fully covariant macroscopic gravity [5]; Buchert’s approach of averaging the scalar parts of Einstein’s equations [6, 7] and the perturbation techniques proposed by Kolb et. al. [8]. Based on the framework developed by Buchert it has been argued by Räsänen [9] that backreaction from inhomogeneities from the era of structure formation could lead to an accelerated expansion of the Universe. The Buchert framework from a different perspective developed by Wiltshire [10] also leads to an apparent acceleration due to the different lapse of time in underdense and overdense regions.

Backreaction from inhomogeneities provides an interesting platform for investigating the issue of acceleration in the current epoch without invoking additional physics, since the effects of backreaction gain strength as the inhomogeneities develop into structures around the present era. It needs to be mentioned here that the impact of inhomogeneities on observables [11, 12] of an overall homogeneous FRW model has been debated in the literature [13]. Similar questions have also arisen with regard to the magnitude of backreaction modulated by the effect of shear between overdense and underdense regions [14]. While further investigations with the input of data from future observational probes are required for a conclusive picture to emerge, recent studies [6–10, 13, 15, 16] have provided a strong motivation for exploring further the role of inhomogeneities in the evolution of the present Universe.

The backreaction scenario within the Buchert framework [6, 15, 16] has been recently studied by us from new perspective, *viz.*, the effect of the event horizon on cosmological backreaction [17]. The acceleration of the universe leads to a future event horizon from beyond which it is not possible for any signal to reach us. The currently accelerating epoch dictates the existence of an event horizon since the transition from the previously matter-dominated decelerating expansion. Since backreaction is evaluated from the global distribution of matter inhomogeneities, the event horizon demarcates the spatial regions which are causally connected to us, and hence impact the evolution of our part of the Universe. By con-

*nilok@bose.res.in

†archan@bose.res.in

sidering the Buchert framework with the explicit presence of an event horizon during the present accelerating era, our results [17] indicated the possibility of a transition to a future decelerated era.

In the present paper we perform a comprehensive analysis of various aspects of the above model for the future evolution of our universe in the presence of cosmic inhomogeneities. We consider the universe as a global domain \mathcal{D} which is large enough to have a scale of homogeneity to be associated with it. This global domain \mathcal{D} is then further partitioned into overdense and underdense regions called \mathcal{M} and \mathcal{E} respectively, following the approach in [16]. In this setup we explore the future evolution of the universe and then compare the results to those that are obtained when the effect the event horizon is taken into account. In this manner we are able to demarcate the regions in parameter space for which the effect of backreaction from inhomogeneities causes the global acceleration to first slow down, and then ensures the onset of another future decelerating era.

The paper is organized as follows. In Section II we briefly recapitulate the essential details of the Buchert framework [6, 7, 15] including the two-scale model of inhomogeneities presented in [16]. Next, in Section III we follow the approach of [16] and investigate the future evolution of the universe assuming its present stage of global acceleration. We then illustrate the effects of the event horizon by first assuming an exponential expansion for the universe, and later analyzing numerically the evolution equations in Section IV. Subsequently, in Section V we perform a quantitative comparison of various dynamical features of our model in the presence of an explicit event horizon [17] with the future evolution as obtained within the standard Buchert framework [16]. Finally, we summarize our results and make some concluding remarks in Section V.

II. THE BACKREACTION FRAMEWORK

A. Averaged Einstein equations

In the framework developed by Buchert [6, 7, 15, 16] for the Universe filled with an irrotational fluid of dust, the space-time is foliated into flow-orthogonal hypersurfaces featuring the line-element

$$ds^2 = -dt^2 + g_{ij}dX^i dX^j \quad (1)$$

where the proper time t labels the hypersurfaces and X^i are Gaussian normal coordinates (locating free-falling fluid elements or generalized fundamental observers) in the hypersurfaces, and g^{ij} is the full inhomogeneous three metric of the hypersurfaces of constant proper time. The framework is applicable to perfect fluid matter models.

For a compact spatial domain \mathcal{D} , comoving with the fluid, there is one fundamental quantity characterizing it

and that is its volume. This volume is given by

$$|\mathcal{D}|_g = \int_{\mathcal{D}} d\mu_g \quad (2)$$

where $d\mu_g = \sqrt{{}^{(3)}g}(t, X^1, X^2, X^3)dX^1 dX^2 dX^3$. From the domain's volume one may define a scale-factor

$$a_{\mathcal{D}}(t) = \left(\frac{|\mathcal{D}|_g}{|\mathcal{D}|_g} \right)^{1/3} \quad (3)$$

that encodes the average stretch of all directions of the domain.

Using the Einstein equations, with a pressure-less fluid source, we get the following equations [6, 15, 16]

$$3\frac{\ddot{a}_{\mathcal{D}}}{a_{\mathcal{D}}} = -4\pi G \langle \rho \rangle_{\mathcal{D}} + \mathcal{Q}_{\mathcal{D}} + \Lambda \quad (4)$$

$$3H_{\mathcal{D}}^2 = 8\pi G \langle \rho \rangle_{\mathcal{D}} - \frac{1}{2} \langle \mathcal{R} \rangle_{\mathcal{D}} - \frac{1}{2} \mathcal{Q}_{\mathcal{D}} + \Lambda \quad (5)$$

$$0 = \partial_t \langle \rho \rangle_{\mathcal{D}} + 3H_{\mathcal{D}} \langle \rho \rangle_{\mathcal{D}} \quad (6)$$

Here the average of the scalar quantities on the domain \mathcal{D} is defined as,

$$\langle f \rangle_{\mathcal{D}}(t) = \frac{\int_{\mathcal{D}} f(t, X^1, X^2, X^3) d\mu_g}{\int_{\mathcal{D}} d\mu_g} = |\mathcal{D}|_g^{-1} \int_{\mathcal{D}} f d\mu_g \quad (7)$$

and where ρ , \mathcal{R} and $H_{\mathcal{D}}$ denote the local matter density, the Ricci-scalar of the three-metric g_{ij} , and the domain dependent Hubble rate $H_{\mathcal{D}} = \dot{a}_{\mathcal{D}}/a_{\mathcal{D}}$ respectively. The kinematical backreaction $\mathcal{Q}_{\mathcal{D}}$ is defined as

$$\mathcal{Q}_{\mathcal{D}} = \frac{2}{3} \left(\langle \theta^2 \rangle_{\mathcal{D}} - \langle \theta \rangle_{\mathcal{D}}^2 \right) - 2\sigma_{\mathcal{D}}^2 \quad (8)$$

where θ is the local expansion rate and $\sigma^2 = 1/2\sigma_{ij}\sigma^{ij}$ is the squared rate of shear. It should be noted that $H_{\mathcal{D}}$ is defined as $H_{\mathcal{D}} = 1/3 \langle \theta \rangle_{\mathcal{D}}$. $\mathcal{Q}_{\mathcal{D}}$ encodes the departure from homogeneity and for a homogeneous domain its value is zero.

One also has an integrability condition that is necessary to yield (5) from (4) and that relation reads as

$$\frac{1}{a_{\mathcal{D}}^6} \partial_t (a_{\mathcal{D}}^6 \mathcal{Q}_{\mathcal{D}}) + \frac{1}{a_{\mathcal{D}}^2} \partial_t (a_{\mathcal{D}}^2 \langle \mathcal{R} \rangle_{\mathcal{D}}) = 0 \quad (9)$$

From this equation we see that the evolution of the backreaction term, and hence extrinsic curvature inhomogeneities, is coupled to the average intrinsic curvature. Unlike the FRW evolution equations where the curvature term is restricted to an $a_{\mathcal{D}}^{-2}$ behaviour, here it is more dynamical because it can be any function of $a_{\mathcal{D}}$.

B. Separation formulae for arbitrary partitions

The ‘‘global’’ domain \mathcal{D} is assumed to be separated into subregions \mathcal{F}_{ℓ} , which themselves consist of elementary

space entities $\mathcal{F}_\ell^{(\alpha)}$ that may be associated with some averaging length scale. In mathematical terms $\mathcal{D} = \cup_\ell \mathcal{F}_\ell$, where $\mathcal{F}_\ell = \cup_\alpha \mathcal{F}_\ell^{(\alpha)}$ and $\mathcal{F}_\ell^{(\alpha)} \cap \mathcal{F}_m^{(\beta)} = \emptyset$ for all $\alpha \neq \beta$ and $\ell \neq m$. The average of the scalar valued function f on the domain \mathcal{D} (7) may then be split into the averages of f on the subregions \mathcal{F}_ℓ in the form,

$$\langle f \rangle_{\mathcal{D}} = \sum_\ell |\mathcal{D}|_g^{-1} \sum_\alpha \int_{\mathcal{F}_\ell^{(\alpha)}} f d\mu_g = \sum_\ell \lambda_\ell \langle f \rangle_{\mathcal{F}_\ell} \quad (10)$$

where $\lambda_\ell = |\mathcal{F}_\ell|_g/|\mathcal{D}|_g$, is the volume fraction of the subregion \mathcal{F}_ℓ . The above equation directly provides the expression for the separation of the scalar quantities ρ , \mathcal{R} and $H_{\mathcal{D}} = 1/3 \langle \theta \rangle_{\mathcal{D}}$. However, $\mathcal{Q}_{\mathcal{D}}$, as defined in (8), does not split in such a simple manner due to the $\langle \theta \rangle_{\mathcal{D}}^2$ term. Instead the correct formula turns out to be

$$\mathcal{Q}_{\mathcal{D}} = \sum_{\mathcal{D}} \lambda_\ell \mathcal{Q}_\ell + 3 \sum_{\ell \neq m} \lambda_\ell \lambda_m (H_\ell - H_m)^2 \quad (11)$$

where \mathcal{Q}_ℓ and H_ℓ are defined in \mathcal{F}_ℓ in the same way as $\mathcal{Q}_{\mathcal{D}}$ and $H_{\mathcal{D}}$ are defined in \mathcal{D} . The shear part $\langle \sigma^2 \rangle_{\mathcal{F}_\ell}$ is completely absorbed in \mathcal{Q}_ℓ , whereas the variance of the local expansion rates $\langle \theta^2 \rangle_{\mathcal{D}} - \langle \theta \rangle_{\mathcal{D}}^2$ is partly contained in \mathcal{Q}_ℓ but also generates the extra term $3 \sum_{\ell \neq m} \lambda_\ell \lambda_m (H_\ell - H_m)^2$. This is because the part of the variance that is present in \mathcal{Q}_ℓ , namely $\langle \theta^2 \rangle_{\mathcal{F}_\ell} - \langle \theta \rangle_{\mathcal{F}_\ell}^2$ only takes into account points inside \mathcal{F}_ℓ . To restore the variance that comes from combining points of \mathcal{F}_ℓ with others in \mathcal{F}_m , the extra term containing the averaged Hubble rate emerges. Note here that the above formulation of the backreaction holds in the case when there is no interaction between the overdense and the underdense subregions.

Analogous to the scale-factor for the global domain, a scale-factor a_ℓ for each of the subregions \mathcal{F}_ℓ can be defined such that $|\mathcal{D}|_g = \sum_\ell |\mathcal{F}_\ell|_g$, and hence,

$$a_{\mathcal{D}}^3 = \sum_\ell \lambda_{\ell_i} a_{\ell}^3 \quad (12)$$

where $\lambda_{\ell_i} = |\mathcal{F}_{\ell_i}|_g/|\mathcal{D}_i|_g$ is the initial volume fraction of the subregion \mathcal{F}_ℓ . If we now twice differentiate this equation with respect to the foliation time and use the result for \dot{a}_ℓ from (5), we then get the expression that relates the acceleration of the global domain to that of the sub-domains:

$$\frac{\ddot{a}_{\mathcal{D}}}{a_{\mathcal{D}}} = \sum_\ell \lambda_\ell \frac{\ddot{a}_\ell(t)}{a_\ell(t)} + \sum_{\ell \neq m} \lambda_\ell \lambda_m (H_\ell - H_m)^2 \quad (13)$$

Following the simplifying assumption of [16] (which captures the essential physics), we work with only two subregions. Clubbing those parts of \mathcal{D} which consist of initial overdensity as \mathcal{M} (called ‘wall’), and those with initial underdensity as \mathcal{E} (called ‘void’), such that $\mathcal{D} = \mathcal{M} \cup \mathcal{E}$, one obtains $H_{\mathcal{D}} = \lambda_{\mathcal{M}} H_{\mathcal{M}} + \lambda_{\mathcal{E}} H_{\mathcal{E}}$, with similar expressions for $\langle \rho \rangle_{\mathcal{D}}$ and $\langle \mathcal{R} \rangle_{\mathcal{D}}$, and

$$\frac{\ddot{a}_{\mathcal{D}}}{a_{\mathcal{D}}} = \lambda_{\mathcal{M}} \frac{\ddot{a}_{\mathcal{M}}}{a_{\mathcal{M}}} + \lambda_{\mathcal{E}} \frac{\ddot{a}_{\mathcal{E}}}{a_{\mathcal{E}}} + 2\lambda_{\mathcal{M}}\lambda_{\mathcal{E}}(H_{\mathcal{M}} - H_{\mathcal{E}})^2 \quad (14)$$

Here $\sum_\ell \lambda_\ell = \lambda_{\mathcal{M}} + \lambda_{\mathcal{E}} = 1$, with $\lambda_{\mathcal{M}} = |\mathcal{M}|/|\mathcal{D}|$ and $\lambda_{\mathcal{E}} = |\mathcal{E}|/|\mathcal{D}|$.

III. FUTURE EVOLUTION WITHIN THE BUCHERT FRAMEWORK

We now try to see what happens to the evolution of the universe once the present stage of acceleration sets in. Note, henceforth, we do not need to necessarily assume that the acceleration is due to backreaction [9, 16]. For the purpose of our present analysis, it suffices to consider the observed accelerated phase of the universe [4] that could occur due to any of a variety of mechanisms [3].

Since the global domain \mathcal{D} is large enough for a scale of homogeneity to be associated with it, one can write,

$$|\mathcal{D}|_g = \int_{\mathcal{D}} \sqrt{-g} d^3 X = f(r) a_F^3(t) \quad (15)$$

where $f(r)$ is a function of the FRW comoving radial coordinate r . It then follows that

$$a_{\mathcal{D}} \approx \left(\frac{f(r)}{|\mathcal{D}_i|_g} \right)^{1/3} a_F \equiv c_F a_F, \quad (16)$$

and hence the volume average scale-factor $a_{\mathcal{D}}$ and the FRW scale-factor a_F are related by $a_{\mathcal{D}} \approx c_F a_F$, where c_F is a constant in time. Thus, $H_F \approx H_{\mathcal{D}}$, where H_F is the FRW Hubble parameter associated with \mathcal{D} . Though in general $H_{\mathcal{D}}$ and H_F could differ on even large scales [16], the above approximation is valid for small metric perturbations.

Following the Buchert framework [6, 16] as discussed above, the global domain \mathcal{D} is divided into a collection of overdense regions $\mathcal{M} = \cup_j \mathcal{M}^j$, with total volume $|\mathcal{M}|_g = \sum_j |\mathcal{M}^j|_g$, and underdense regions $\mathcal{E} = \cup_j \mathcal{E}^j$ with total volume $|\mathcal{E}|_g = \sum_j |\mathcal{E}^j|_g$. Assuming that the scale-factors of the regions \mathcal{E}^j and \mathcal{M}^j are, respectively, given by $a_{\mathcal{E}^j} = c_{\mathcal{E}^j} t^\alpha$ and $a_{\mathcal{M}^j} = c_{\mathcal{M}^j} t^\beta$ where α , β , $c_{\mathcal{E}^j}$ and $c_{\mathcal{M}^j}$ are constants, one has

$$a_{\mathcal{E}}^3 = c_{\mathcal{E}}^3 t^{3\alpha}; \quad a_{\mathcal{M}}^3 = c_{\mathcal{M}}^3 t^{3\beta} \quad (17)$$

where $c_{\mathcal{E}}^3 = \frac{\sum_j c_{\mathcal{E}^j}^3 |\mathcal{E}^j|_g}{|\mathcal{E}|_g}$ is a new constant, and similarly for $c_{\mathcal{M}}$. The volume fraction of the subdomain \mathcal{M} is given by $\lambda_{\mathcal{M}} = \frac{|\mathcal{M}|_g}{|\mathcal{D}|_g}$, which can be rewritten in terms of the corresponding scale factors as $\lambda_{\mathcal{M}} = \frac{a_{\mathcal{M}}^3 |\mathcal{M}_i|_g}{a_{\mathcal{D}}^3 |\mathcal{D}_i|_g}$. We therefore find that the global acceleration equation (14) becomes

$$\begin{aligned} \frac{\ddot{a}_{\mathcal{D}}}{a_{\mathcal{D}}} &= \frac{g_{\mathcal{M}_h}^3 t^{3\beta}}{a_{\mathcal{D}}^3} \frac{\beta(\beta-1)}{t^2} + \left(1 - \frac{g_{\mathcal{M}_h}^3 t^{3\beta}}{a_{\mathcal{D}}^3} \right) \frac{\alpha(\alpha-1)}{t^2} \\ &+ 2 \frac{g_{\mathcal{M}_h}^3 t^{3\beta}}{a_{\mathcal{D}}^3} \left(1 - \frac{g_{\mathcal{M}_h}^3 t^{3\beta}}{a_{\mathcal{D}}^3} \right) \left(\frac{\beta}{t} - \frac{\alpha}{t} \right)^2 \end{aligned} \quad (18)$$

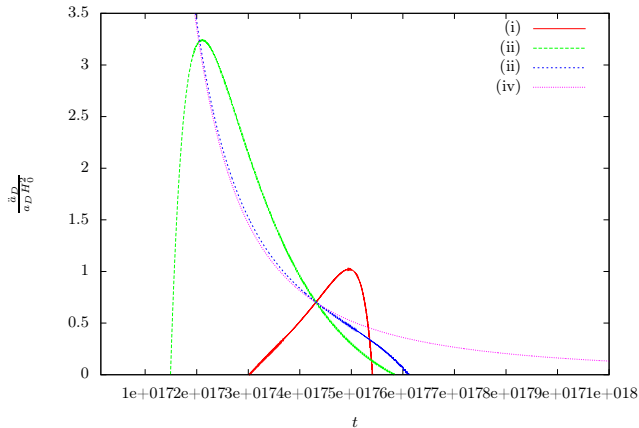


Figure 1: Global acceleration parameter plotted vs. time. The parameter values used are: (i) $\alpha = 0.995$, $\beta = 0.5$, (ii) $\alpha = 0.984$, $\beta = 0.5$, (iii) $\alpha = 1.02$, $\beta = 0.66$, (iv) $\alpha = 1.02$, $\beta = 0.66$. (The curves (i) and (iii) correspond to the case when an event horizon is included in the analysis in Section IV).

where $g_{\mathcal{M}_h}$ is a constant. We obtain numerical solutions of the above equation for various parameter values (see curves (ii) and (iv) of Fig.1). We later compare these with the solutions of the model with an explicit event horizon studied in Section IV.

A. Backreaction and Scalar Curvature

It is of interest to study separately the behaviour of the backreaction term in the Buchert model [6, 16]. The backreaction $Q_{\mathcal{D}}$ is obtained from (4) to be

$$Q_{\mathcal{D}} = 3\frac{\ddot{a}_{\mathcal{D}}}{a_{\mathcal{D}}} + 4\pi G \langle \rho \rangle_{\mathcal{D}} \quad (19)$$

Note that we are not considering the presence of any cosmological constant Λ as shown in (4). We can assume that $\langle \rho \rangle_{\mathcal{D}}$ behaves like the matter energy density, i.e. $\langle \rho \rangle_{\mathcal{D}} = \frac{c_{\rho}}{a_{\mathcal{D}}^3}$, where c_{ρ} is a constant. Now, observations tell us that the current matter energy density fraction (baryonic and dark matter) is about 27% and that of dark energy is about 73%. Assuming the dark energy density to be of the order of $10^{-48} (GeV)^4$, we get $\rho_{\mathcal{D}_0} \simeq 3.699 \times 10^{-49} (GeV)^4$. Thus, using the values for the global acceleration computed numerically, the future evolution of the backreaction term $Q_{\mathcal{D}}$ can also be computed (see curves (ii) and (iv) of Fig.2, where we have plotted the backreaction density fraction $\Omega_{\mathcal{Q}}^{\mathcal{D}} = -\frac{Q_{\mathcal{D}}}{6H_{\mathcal{D}}^2}$). Once we compute the backreaction it is straightforward to calculate the scalar curvature $\langle \mathcal{R} \rangle_{\mathcal{D}}$ as

$$\langle \mathcal{R} \rangle_{\mathcal{D}} = 16\pi G \langle \rho \rangle_{\mathcal{D}} - Q_{\mathcal{D}} - 6H_{\mathcal{D}}^2 \quad (20)$$

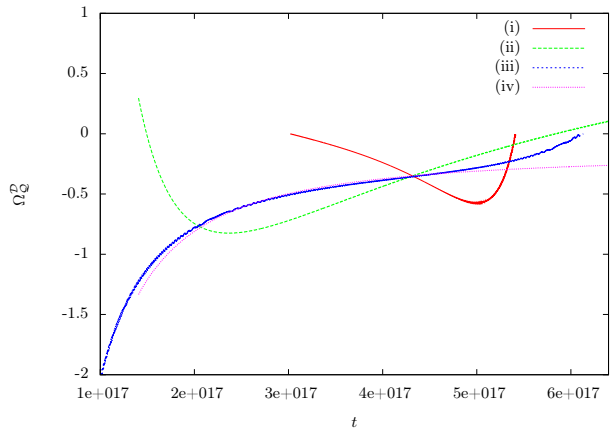


Figure 2: Global backreaction density fraction vs. time. The parameter values used are the same as in Fig. 1.

B. Effective Equation of State

To point out the analogy with the Friedmann equations one may write (4) and (5) as

$$\begin{aligned} 3\frac{\ddot{a}_{\mathcal{D}}}{a_{\mathcal{D}}} &= -4\pi G (\rho_{eff}^{\mathcal{D}} + 3p_{eff}^{\mathcal{D}}) \\ 3H_{\mathcal{D}}^2 &= 8\pi G \rho_{eff}^{\mathcal{D}} \end{aligned} \quad (21)$$

where the effective energy density and pressure are defined as

$$\begin{aligned} \rho_{eff}^{\mathcal{D}} &= \langle \rho \rangle_{\mathcal{D}} - \frac{1}{16\pi G} Q_{\mathcal{D}} - \frac{1}{16\pi G} \langle \mathcal{R} \rangle_{\mathcal{D}} \\ p_{eff}^{\mathcal{D}} &= -\frac{1}{16\pi G} Q_{\mathcal{D}} + \frac{1}{48\pi G} \langle \mathcal{R} \rangle_{\mathcal{D}} \end{aligned} \quad (22)$$

Note that as in (19), here also we are not considering the presence of any cosmological constant Λ . In this sense, $Q_{\mathcal{D}}$ and $\langle \mathcal{R} \rangle_{\mathcal{D}}$ may be combined to some kind of dark fluid component that is commonly referred to as X -matter. One quantity characterizing this X -matter is its equation of state given by

$$w_{\Lambda,eff}^{\mathcal{D}} = \frac{p_{eff}^{\mathcal{D}}}{\rho_{eff}^{\mathcal{D}} - \langle \rho \rangle_{\mathcal{D}}} = \frac{Q_{\mathcal{D}} - \frac{1}{3}\langle \mathcal{R} \rangle_{\mathcal{D}}}{Q_{\mathcal{D}} + \langle \mathcal{R} \rangle_{\mathcal{D}}} = \frac{\Omega_{\mathcal{Q}}^{\mathcal{D}} - \frac{1}{3}\Omega_{\mathcal{R}}^{\mathcal{D}}}{\Omega_{\mathcal{Q}}^{\mathcal{D}} + \Omega_{\mathcal{R}}^{\mathcal{D}}} \quad (23)$$

which is an effective one due to the fact that backreaction and curvature give rise to effective energy density and pressure. We again plot this effective equation of state by computing its value numerically (see curves (ii) and (iv) of Fig.3), and in the next Section we compare the results with those obtained by considering the effect of an event horizon.

IV. EFFECT OF EVENT HORIZON

In the previous section we have performed a detailed analysis of the future evolution of an accelerating uni-

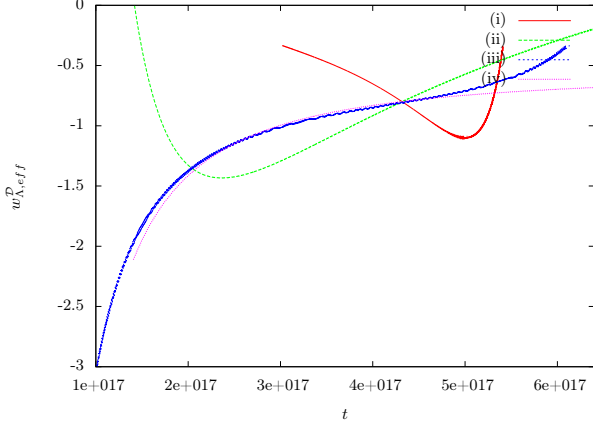


Figure 3: Effective equation of state vs. time. The parameter values used are: (i) $\alpha = 0.995$, $\beta = 0.5$, (ii) $\alpha = 0.984$, $\beta = 0.5$, (iii) $\alpha = 1.02$, $\beta = 0.66$, (iv) $\alpha = 1.02$, $\beta = 0.66$

verse by calculating the effect of backreaction from inhomogeneities on the various dynamical quantities within the context of the Buchert framework. As mentioned earlier, an accelerated expansion dictates the formation of an event horizon, and our earlier analysis may be interpreted as a tacit assumption of a horizon scale being set by the scale of homogeneity labelled by the global scale-factor, i.e. $r_h \approx a_{\mathcal{D}}$. In the present section we introduce explicitly such an event horizon. Given that we are undergoing a stage of acceleration since transition from an era of structure formation, our aim here is to explore the subsequent evolution of the Universe due to the effects of backreaction in presence of the cosmic event horizon. Though, in general, spatial and light cone distances and corresponding accelerations could be different, as shown explicitly in the framework of Lemaitre–Tolman–Bondi (LTB) models [18], an approximation for the event horizon which forms at the onset of acceleration could be defined by

$$r_h = a_{\mathcal{D}} \int_t^{\infty} \frac{dt'}{a_{\mathcal{D}}(t')} \quad (24)$$

in the same spirit as $a_{\mathcal{D}} = c_F a_F$.

Since an event horizon forms only those regions of \mathcal{D} that are within the event horizon are accessible to us. Hence, in this case an apparent volume fraction $\lambda_{\mathcal{M}_h} = \frac{a_{\mathcal{M}}^3 |\mathcal{M}_i|_g}{\frac{4}{3} \pi r_h^3}$ is introduced. From (17) it follows that

$$\lambda_{\mathcal{M}_h} = \frac{c_{\mathcal{M}_h}^3 t^{3\beta}}{r_h^3} \quad (25)$$

where $c_{\mathcal{M}_h}^3 = c_{\mathcal{M}}^3 |\mathcal{M}_i|_g / \frac{4}{3} \pi$ is a constant. Normalizing the total accessible volume in the presence of the event horizon, we can write

$$\lambda_{\mathcal{E}_h} = 1 - \lambda_{\mathcal{M}_h} \quad (26)$$

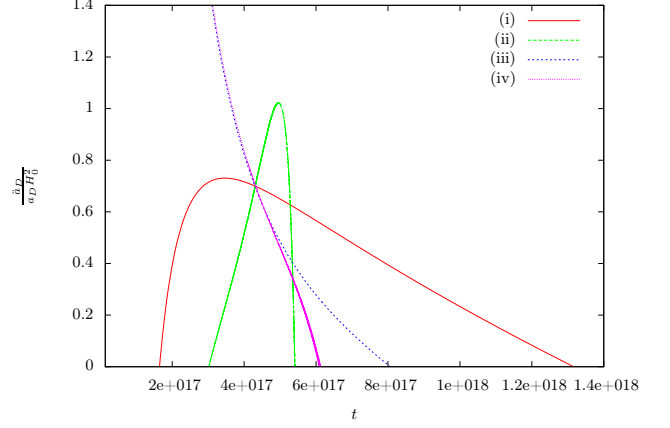


Figure 4: The dimensionless global acceleration parameter plotted vs. time (s). The parameter values for curves (i) and (ii) are $\alpha = 0.995$, $\beta = 0.5$, and for curves (iii) and (iv) are $\alpha = 1.02$, $\beta = 0.66$.

where $\lambda_{\mathcal{E}_h}$ is the apparent volume fraction for the sub-domain \mathcal{E} . It hence follows that the global acceleration equation (14) is now given by

$$\frac{\ddot{a}_{\mathcal{D}}}{a_{\mathcal{D}}} = \frac{c_{\mathcal{M}_h}^3 t^{3\beta} \beta(\beta-1)}{r_h^3 t^2} + \left(1 - \frac{c_{\mathcal{M}_h}^3 t^{3\beta}}{r_h^3}\right) \frac{\alpha(\alpha-1)}{t^2} + 2 \frac{c_{\mathcal{M}_h}^3 t^{3\beta}}{r_h^3} \left(1 - \frac{c_{\mathcal{M}_h}^3 t^{3\beta}}{r_h^3}\right) \left(\frac{\beta}{t} - \frac{\alpha}{t}\right)^2 \quad (27)$$

In order to obtain the future evolution of the universe with backreaction in presence of the event horizon, one has to solve the above equation for the scale-factor with the event horizon r_h given by (24).

Though we will eventually obtain numerical solutions of the above integro-differential equations, it is instructive to first obtain some physical insight of the evolution by taking recourse to a simple approximation. To this end, let us for the moment model the onset of the present acceleration of the Universe by an exponential expansion, keeping our analysis close to observations. Specifically, we set $a_{\mathcal{D}} \propto \exp(H_{\mathcal{D}} t)$ in equation (24) only. Using $H_F = H_{\mathcal{D}}$, where H_F is the FRW Hubble parameter associated with \mathcal{D} , it follows that $r_h = H_F^{-1}$, a constant which we substitute in equation (27). With this substitution, the global acceleration $\ddot{a}_{\mathcal{D}}$ vanishes at times given by

$$t^{3\beta} = [(3\beta - \alpha - 1) \pm \sqrt{(3\beta - \alpha - 1)^2 + 8\alpha(\alpha - 1)}] \quad (28)$$

The scalefactor of the ‘wall’ grows as t^β , where $1/2 \leq \beta \leq 2/3$. Equation (28) corresponds to real time solutions for $\alpha \geq \frac{1}{3} [(\beta + 1) + 2\sqrt{2\beta(1 - \beta)}]$.

Now, let us consider the following two cases separately.

Case I: $\alpha < 1$ and $\beta \leq 2/3$. There exist two real solutions of (28) corresponding to two values of time when

the global acceleration vanishes. In Fig. 4, we plot a dimensionless global acceleration parameter $\frac{\ddot{a}_{\mathcal{D}}}{a_{\mathcal{D}}H_0^2}$ with time using equation (27). The curve (i) corresponds to this case showing that the Universe first enters the epoch of acceleration due to backreaction, which subsequently slows down and finally vanishes at the onset of another decelerating era in the future.

Case II: $\alpha \geq 1$ and $\beta \leq 2/3$. From (28) it follows that there is only one real solution (minus sign for the square root). This case models the Universe which accelerates due to some other mechanism (not backreaction), but subsequently enters an epoch of deceleration due to backreaction of inhomogeneities in the presence of the event horizon [see curve (iii) of Fig. 4].

The plots in Fig. 4 have been done taking the standard values of the parameters $r_h = H_{\mathcal{D}_0}^{-1} = 4.36 \times 10^{17} s$, while choosing the appropriate range for the parameters α and β , as given in the figure caption. Based on the N-body simulation values used in [16], we also take $\lambda_{\mathcal{M}_{h_0}} = 0.09$.

We now study the acceleration (27) numerically without assuming a priori any behaviour for the horizon. Keeping with the spirit of our analysis, we assume that the Universe has entered the accelerated stage and thus a cosmic event horizon has formed. This ensures that r_h defined by (24) will be finite valued, enabling us to replace the integral equation (24) by

$$\dot{r}_h = \frac{\dot{a}_{\mathcal{D}}}{a_{\mathcal{D}}} r_h - 1 \quad (29)$$

Thus, the evolution of the scale-factor is now governed by the set of coupled differential equations (27) and (29). We numerically integrate these equations by using as an 'initial condition' the observational constraint $q_0 \approx -0.7$, where q_0 is the current value of the deceleration parameter (we also used this condition to plot the curves for the exponential case), and using the solution for the scale-factor plot the global acceleration versus time in Fig. 4 (curves (ii) and (iv) [thus, all the curves in Fig. 4 are set to intersect at the point (t_0, q_0)]. The values of the other parameters including α and β are chosen to be the same as in the corresponding curves of the exponential case. Curves (ii) and (iv) in Fig. 4 are drawn from the numerical solutions where curve (ii) corresponds to the case where $\alpha < 1$ and curve (iv) corresponds to the case where $\alpha \geq 1$. For $\alpha < 1$ we see that for the numerical case (curve (ii)) the acceleration decreases much more sharply than the analytic (exponential) case (curve (i)). In contrast, for $\alpha > 1$, the acceleration which has only one transition between acceleration and deceleration in the future, looks much more similar for both the (exponential and numerical) cases. Therefore, it turns out that the exponential expansion for the universe is a much better approximation when we have $\alpha > 1$. The differences in the various slopes and also in the scale for the dimensionless global acceleration parameter in the two cases arise as a result of the approximation of constant horizon used in the former, as well as due to the choice of the condition $q_0 \approx -0.7$ used in both the cases.

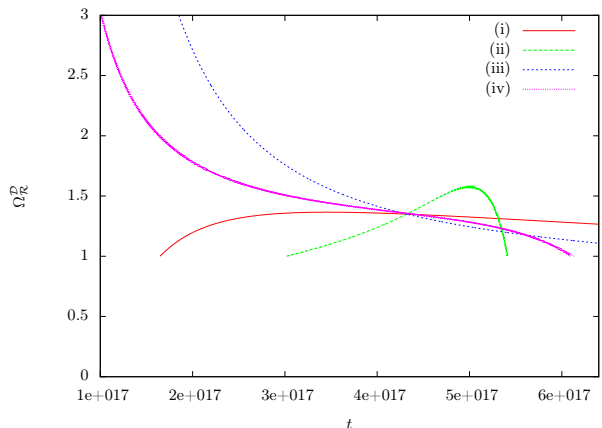


Figure 5: Global scalar curvature density fraction, $\Omega_{\mathcal{R}}^{\mathcal{D}}$ plotted vs. time. The parameter values for curves (i) and (ii) are $\alpha = 0.995$, $\beta = 0.5$, and for curves (iii) and (iv) are $\alpha = 1.02$, $\beta = 0.66$.

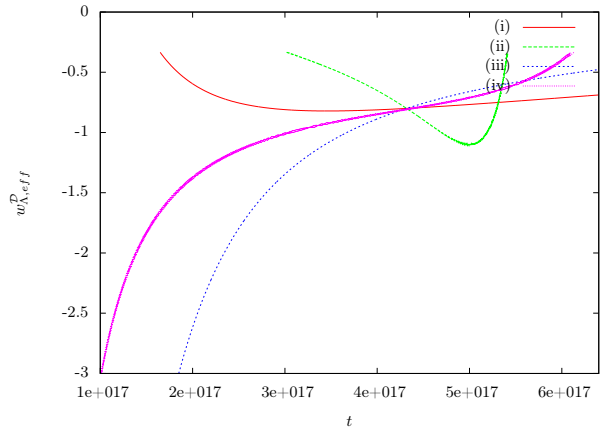


Figure 6: Effective equation of state, $w_{\Lambda,eff}^{\mathcal{D}}$ plotted vs. time. The parameter values for curves (i) and (ii) are $\alpha = 0.995$, $\beta = 0.5$, and for curves (iii) and (iv) are $\alpha = 1.02$, $\beta = 0.66$.

We now compute the backreaction $Q_{\mathcal{D}}$ for this model, using Eq. (19). Once we compute the backreaction it is straightforward to obtain the scalar curvature $\langle \mathcal{R} \rangle_{\mathcal{D}}$ numerically, as was done in the previous section for the model without the event horizon. In Fig. 5 we have plotted the scalar curvature density fraction $\Omega_{\mathcal{R}}^{\mathcal{D}} = -\frac{\langle \mathcal{R} \rangle_{\mathcal{D}}}{6H_{\mathcal{D}}^2}$. The curves (i) and (iii) correspond to the exponential case and curves (ii) and (iv) correspond to the numerical case. We observe from Fig. 5 is that the scalar curvature $\langle \mathcal{R} \rangle_{\mathcal{D}}$ turns out to be negative when the Universe is in an accelerated phase, which is what we expect from our knowledge of FRW cosmology. For $\alpha < 1$ the curvature increases to a maximum and then decreases, but for $\alpha > 1$ the curvature density keeps on monotonically decreasing. Just like we observed in the acceleration plot (Fig. 4), here also the assumption of exponential expansion is a much better approximation when we have $\alpha > 1$.

We next compute the effective equation of state using Eq.(23). We see that for the duration of positive acceleration the equation of state remains negative. For $\alpha < 1$ the equation of state first reaches a minimum and then keeps on rising. This rise is much more rapid for the numerical case (curve (ii)). For $\alpha > 1$ the equation of state keeps on rising monotonically. In this case it is quite apparent that the acceleration of the universe is caused by something other than backreaction, since the equation of state starts from large negative values. Here also we find that the assumption of exponential expansion is a much more better approximation when $\alpha > 1$.

V. DISCUSSIONS

Let us now compare the nature of acceleration of the Universe for the two models described respectively, in Sections III and IV. The global acceleration for the two models have been plotted in Fig. 1. Here curves (i) and (iii) are for the case when an event horizon is included, and curves (ii) and (iv) correspond to the case without an event horizon. For $\alpha < 1$ we see that the acceleration reaches a much greater value when no event horizon is present and that too very quickly, but decreases much more gradually than when an event horizon is included. This behaviour could be due to the fact that the inclusion of the event horizon somehow limits the global volume of domain \mathcal{D} in such a way that the available volume of the underdense region \mathcal{E} is lesser than when an event horizon is not included. This causes the overdense region \mathcal{M} to start dominating much earlier and thus causing global deceleration much more quickly. When $\alpha > 1$ the acceleration goes asymptotically to zero when an event horizon is not included (curve (iv)), which is contrary to the case with an event horizon because there the acceleration always becomes negative in the future whether $\alpha < 1$ or $\alpha > 1$. In fact here also we can see that when we include an event horizon in our calculations then there is much more rapid deceleration, the reason for which is mentioned above. Initially the curves for the two case are almost identical, but later on they diverge due to the faster deceleration for the case when an event horizon is included.

A similar comparison of the backreaction for the two models is presented in Fig. 2. From the expression of $\Omega_{\mathcal{Q}}^{\mathcal{D}}$ and (8) it can be seen that the backreaction will be dominated by the variance of the local expansion rate θ . Here we observe that even for the model where an event horizon is not included, $\Omega_{\mathcal{Q}}^{\mathcal{D}}$ is negative for the duration over which the acceleration is positive (although $\Omega_{\mathcal{Q}}^{\mathcal{D}}$ is positive at the extreme edges). For $\alpha < 1$ the backreaction density first reaches a minimum and then keeps on rising, this rise being much more rapid for the case where an event horizon is included (curve (i)). For $\alpha > 1$ the backreaction density keeps on rising monotonically. Here curves for both the models are initially very similar but later on they diverge.

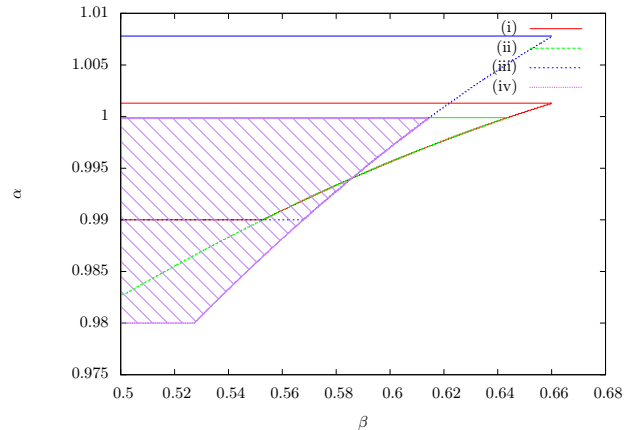


Figure 7: The range of parameters α and β for which future deceleration takes place, shown within the respective contours for the curves (i) and (iii) corresponding to the case with an event horizon, and the curves (ii) and (iv) corresponding to the case where an event horizon is not considered. The value of $\lambda_{\mathcal{M}0}$ for the curves (i) and (ii) is 0.15 and for curves (iii) and (iv) is 0.2. The shaded region corresponds to the curve (iv) demarcating the parameter space for this case when acceleration vanishes in finite future time.

We next consider the effective equation of state $w_{\Lambda,eff}^{\mathcal{D}}$ (Fig. 3). It remains negative for the entire duration over which the acceleration is positive. For $\alpha < 1$, $w_{\Lambda,eff}^{\mathcal{D}}$ first reaches a minimum and then keeps on rising. The falling to the minimum is much faster for the model where an event horizon is not included (curve (ii)) and the increase from the minimum being much faster for the case where an event horizon is included (curve(i)). For $\alpha > 1$ the curves for the two cases are very similar initially (again like backreaction plots) but later on they diverge.

From our analysis so far it is clear that the acceleration of the Universe could become negative in the future for certain values of the parameters α and β , which represent the growth rates of the scale factors corresponding to the void and wall, respectively. The range of values of α and β for which a future transition to deceleration is possible, is depicted in Fig. 7. We provide a contour plot of α versus β demarcating the range in parameter space (inside of the contours) for which acceleration vanishes in finite future time. We see that initially the curves for the model with an event horizon (curves (i) and (iii)) have the same value of α for various values of β . But later on when the values of α begin to change then the curves for the two models (with and without event horizon) merge. Since the acceleration has no chance of becoming negative when we have $\alpha > 1$, and for the case with no event horizon (the acceleration then goes asymptotically to zero), we therefore get the maximum limit of α for this case depicted by the line $\alpha = 1$.

VI. CONCLUSIONS

To summarize, in this work we have performed a detailed analysis of the various aspects of the future evolution of the presently accelerating universe in the presence of matter inhomogeneities. The backreaction of inhomogeneities on the global evolution is calculated within the context of the Buchert framework for a two-scale non-interacting void-wall model [6, 7, 15, 16]. We first analyze the future evolution using the Buchert framework by computing various dynamical quantities such as the global acceleration, strength of backreaction, scalar curvature and equation of state. Though in this case we do not consider explicitly the effect of the event horizon, it may be argued that a horizon scale is implicitly set by the scale of global homogeneity labelled by the global scale-factor. We show that the Buchert framework allows for the possibility of the global acceleration vanishing at a finite future time, provided that none of the subdomains accelerate individually (both α and β are less than 1).

We next consider in detail a model with an explicit event horizon, first presented in [17]. The observed present acceleration of the universe dictates the occurrence of a future event horizon since the onset of the present accelerating era. It may be noted that though the event horizon is observer dependent, the symmetry of the equation (27) following from (14) ensures that our analysis would lead to similar conclusions for a 'void' centric observer, as it does for a 'wall' centric one. In [17] we had shown that the presence of the cosmic event horizon causes the acceleration to slow down significantly with time. In the present paper in order to understand better the underlying physics behind the slowing down of the global acceleration, we have explored the nature of the global backreaction, scalar curvature and effective equation of state. We have provided a quantitative comparison of the evolution of these dynamical quantities of this model with the case when an event horizon is not included.

Our analysis confirms that the evolution with backreaction from inhomogeneities in the presence of an event

horizon for some time after the onset of the present accelerating epoch in the case when one of the individual subdomains, i.e., the underdense wall, is accelerating on its own, stays close to the standard Λ CDM model (with exponential expansion). On the other hand, in comparison with the model without an event horizon, we find that during the subsequent future evolution the global acceleration decreases more quickly when we include an event horizon. The reason for this effect is that in the latter model an effective reduction of the volume fraction for the void leads to the overdense region starting to dominate much earlier and hence, causes faster deceleration of the universe. One important difference between the acceleration of the two models is that the acceleration does not vanish in finite time, but instead goes asymptotically to zero for $\alpha > 1$ when no event horizon is included. Nonetheless, when $\alpha > 1$, the curves for acceleration, backreaction, scalar curvature, and effective equation of state for both the cases are very similar and only diverge later on. We finally demarcate the region in the parameter space of the growth rates of the void and the wall, where it is possible to obtain a transition to deceleration in the finite future.

Our results indicate the fascinating possibility of backreaction being responsible for not only the present acceleration as shown in earlier works [9, 16], but also leading to a transition to another decelerated era in the future. Another possibility following from our analysis is of the Universe currently accelerating due to a different mechanism [3], but with backreaction [6, 15, 16] later causing acceleration to slow down. Finally, it may be noted that the formalism for obtaining backreaction [6, 7, 15, 16] used here relies on averaging on constant time hypersurfaces. Recently, another procedure based on light-cone averaging has been proposed [19]. Though, the full implications on the cosmological scenario of the latter framework are yet to be deduced, our analysis of including the effect of the event horizon introduces certain elements of lightcone physics in the study of the role of backreaction from inhomogeneities on the global cosmological evolution.

-
- [1] S. Perlmutter, et. al., *Nature* **391**, 51 (1998); A. G. Riess et. al., *Ap. J.* **116**, 1009 (1998); M. Hicken et al., *ApJ*, **700**, 1097 (2009); M. Seikel, D. J. Schwarz, *JCAP* **02**, 024 (2009).
 - [2] S. Weinberg, *Rev. Mod. Phys.*, **61**, 1 (1989); T. Padmanabhan, *Adv. Sci. Lett.* **2**, 174 (2009).
 - [3] V. Sahni, in Papantonopoulos E., ed., *Lecture Notes in Physics Vol. 653, The Physics of the Early Universe*. Springer, Berlin, p. 141 (2004); E. J. Copeland, M. Sami, and S. Tsujikawa, *Int. J. Mod. Phys. D* **15**, 1753 (2006).
 - [4] M. Seikel, D. J. Schwarz, *J. Cosmol. Astropart. Phys.*, **02**, 024 (2009)
 - [5] R. Zalaletdinov, *Gen. Rel. Grav.*, **24**, 1015 (1992); *Gen. Rel. Grav.*, **25**, 673 (1993).
 - [6] T. Buchert, *Gen. Rel. Grav.*, **32**, 105 (2000); T. Buchert, *Gen. Rel. Grav.* **33**, 1381. (2001).
 - [7] T. Buchert, M. Carfora, *Phys. Rev. Lett.* **90**, 031101 (2003).
 - [8] E. W. Kolb, S. Matarrese, A. Notari and A. Riotto, *Phys. Rev. D* **71**, 023524 (2005).
 - [9] S. Rasanen, *J. Cosmol. Astropart. Phys.*, **0402**, 003 (2004); S. Rasanen, *J. Cosmol. Astropart. Phys.*, **0804**, 026 (2008); S. Rasanen, *J. Cosmol. Astropart. Phys.*, **02**, 011 (2009); S. Rasanen, *Phys. Rev. D* **81**, 103512 (2010).
 - [10] D. L. Wiltshire, *New J. Phys.* **9**, 377 (2007); D. L. Wiltshire, *Phys. Rev. Lett.* **99**, 251101 (2007).
 - [11] A. Ishibashi, R. M. Wald, *Classical Quantum Gravity*, **23**, 235 (2006).

- [12] A. Paranjape, T. P. Singh, Phys. Rev. D **78**, 063522 (2008); T. P. Singh, arXiv:1105.3450.
- [13] E. W. Kolb, S. Marra, S. Matarrese, Phys. Rev. D, **78**, 103002 (2008).
- [14] M. Mattsson, T. Mattsson, J. Cosmol. Astropart. Phys. **10**, 021 (2010).
- [15] T. Buchert, M. Carfora, Class. Quant. Grav. **25**, 195001 (2008).
- [16] A. Wiegand, T. Buchert, Phys. Rev. D **82**, 023523 (2010).
- [17] N. Bose, A. S. Majumdar, MNRAS: Letters 418: L45-L48 (2011)
- [18] K. Bolejko, L. Andersson, J. Cosmol. Astropart. Phys., 10, 003 (2008)
- [19] M. Gasperini et al., J. Cosmol. Astropart. Phys., 07, 008 (2011)